

Complex Geometry Creation and Turbulent Conjugate Heat Transfer Modeling

Isaac T. Bodey¹, Rao V. Arimilli¹ and James D. Freels²

¹The University of Tennessee Mechanical, Aerospace and Biomedical Department

²The Oak Ridge National Laboratory

Abstract: The multiphysics capabilities of COMSOL provide the necessary tools to simulate the turbulent thermal-fluid aspects of the High Flux Isotope Reactor (HFIR). Version 4.1, and later, of COMSOL provides three different turbulence models: the standard $k-\epsilon$ closure model, the low Reynolds number (LRN) $k-\epsilon$ model, and the Spalart-Allmaras model. The LRN meets the needs of the nominal HFIR thermal-hydraulic requirements for 2D and 3D simulations. COMSOL also has the capability to create complex geometries. The circular involute fuel plates used in the HFIR require the use of algebraic equations to generate an accurate geometrical representation in the simulation environment.

The best-estimate simulation results show that the maximum fuel plate clad surface temperatures are lower than those predicted by the legacy thermal safety code used at HFIR by approximately 17 K. The best-estimate temperature distribution determined by COMSOL was then used to determine the necessary increase in the magnitude of the power density profile (PDP) to produce a similar clad surface temperature as compared to the legacy thermal safety code. It was determined and verified that a 19% power increase was sufficient to bring the two temperature profiles to relatively good agreement.

Keywords: Turbulence, Conjugate Heat Transfer, Geometry Development

1. Introduction

The Department of Energy (DOE) Global Threat Reduction Initiative (GTRI) is investigating the conversion of the High Flux Isotope Reactor (HFIR), at the Oak Ridge National Laboratory (ORNL), from a high-enriched Uranium (HEU) fueled reactor to a low-enriched Uranium (LEU) fueled reactor (currently scheduled for 2019). The conversion of the HFIR from an HEU fuel

to an LEU fuel is to be implemented with no changes to the external geometrical structure of the core or to the individual fuel plates.

The core geometry is cylindrical with an inner annular fuel array consisting of 171 fuel plates and an outer annular fuel array which consists of 369 fuel plates for a total of 540 fuel plates comprising the HFIR core. The fuel plates of the HFIR are 0.050 inches (1.27 mm) thick and 24 inches (609.6 mm) long in a circular involute geometry with an arc-length of 3.31 inches (84.1 mm) [1]. Each fuel plate has a curved leading edge to aid in the reduction of the pressure drop necessary to maintain operational flow rates. Two adjacent fuel plates form a constant cross-sectional area flow channel with the same dimensions. Figure 1 shows a cutaway view of the HFIR core.

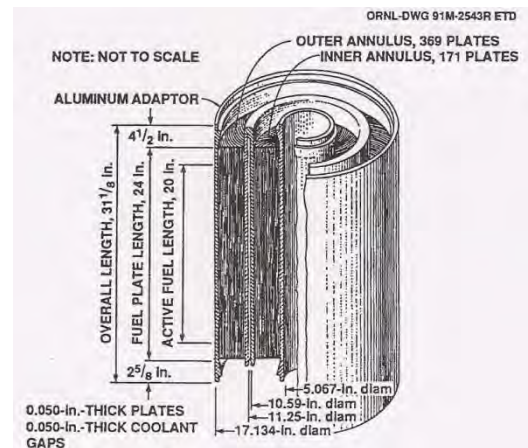


Figure 1. Cutaway View of HFIR Core

The volumetric flow rate through the fueled region of the core is 13,413 gpm (0.846 m³/s) [1]. The Reynolds number, Re , of the flow, based on the hydraulic diameter of a single flow channel and uniform inlet flow velocity, is 69,907 which is well into the turbulent flow regime, i.e. $Re > 2300$.

The core inlet pressure is 482.7 psia (3.33 MPa) with a core pressure drop of 105 psi (0.724

MPa), which yields an exit pressure of 377.7 psia (2.60 MPa) [1]. The saturation temperatures associated with the inlet and exit pressures are 463.33 °F (512.78 K) and 438.88 °F (499.19 K), respectively. The inlet temperature of the core is 128.9 °F (327 K).

The steady-state thermal-hydraulic and structural mechanics characteristics of the HEU HFIR fuel plate have been simulated using a legacy thermal code, hereafter referred to as the Steady State Heat Transfer Code (SSHTC). The SSHTC uses a 2D Cartesian flat plate geometry with the clad surface discretized by a control volume mesh consisting of 31 axial nodes and 11 radial nodes [2], i.e. the thermal interactions of the different materials in the interior of the fuel plate are not simulated.

The SSHTC results in a restrictive model of the HFIR fuel plate in that it does not allow conduction of thermal energy in the axial or span-wise directions, i.e. all thermal energy generated in the fuel plate is passed to the coolant in a direction normal to the clad. As a consequence of this restriction, the SSHTC simulation results are conservative in that they produce higher clad surface temperatures and clad surface heat fluxes than those observed in the core. Another simulation restriction is the use of a Nusselt number correlation to determine the local convection heat transfer coefficient. This restriction eliminates the need to simulate the fluid flow and thus reduces the problem to one of pure conduction.

With respect to safety analysis, the conservative approach used by the SSHTC ensures that the facility will operate within the thermal limits of the reactor core. However, these restrictions also limit the performance potential of the HFIR which will be discussed later.

The COMSOL multiphysics simulation platform is particularly well suited for the turbulent thermal-hydraulic processes that occur in the HFIR during operation. Physical accuracy is increased by the ability to simulate the different physical processes in a single simulation. Before COMSOL could be used to simulate thermal-hydraulic conditions in the core with the LEU fuel, it was first necessary to show that the

software could reproduce the results provided by the SSHTC.

2. COMSOL Conduction Simulation

Since the thermal energy simulated in the SSHTC is only allowed to diffuse in the direction normal to the clad surface, each control volume boundary in the axial and span-wise direction is adiabatic. Thus it is permissible to create a 2D COMSOL simulation geometry (CSG) that represents an interior cross-section of the fuel plate. That is to say the CSG incorporates the interior structure of the fuel plate and the thermal interactions between these components.

The HEU fuel meat in the HFIR fuel plate has a contour relative to the involute arc length. This is shown in Figure 2. A discussion of the LEU fuel plate geometry is given in the Appendix.

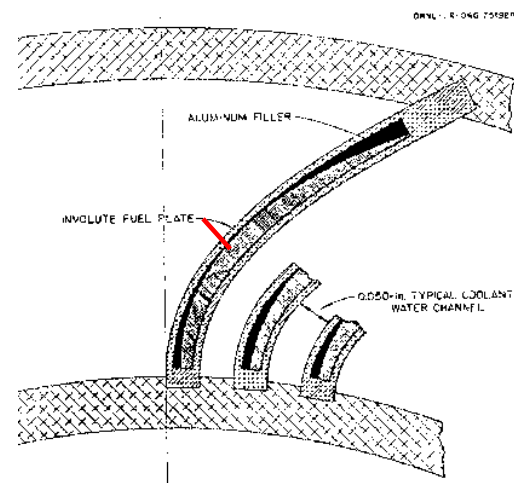


Figure 2. Inner Plate Fuel Meat Contour Relative to the Involute. The red line indicates the 2D slice for the CSG.

The HEU fuel meat consists of 30 wt% U_3O_8 and 1100 Al powders. The CSG represents an axial strip taken at the location of the red line in Figure 2. This strip runs the full 24-inch length of the fuel plate. The dark region of the fuel plate interior is filled with 1100 Al powder and 0.0164 g of B_4C [1], the combination of which constitutes the filler material. This position in the fuel plate was chosen due to the relative

thickness of the filler material with respect to the fuel meat. Since the filler material is thin relative to the fuel meat at this location, the thermal influence of this material will be negligible. Therefore the filler material is not incorporated in the CSG. Removing the filler material from the simulation geometry creates a symmetry plane along the involute arc-length at the center of the fuel meat. The CSG is shown in Figure 3.

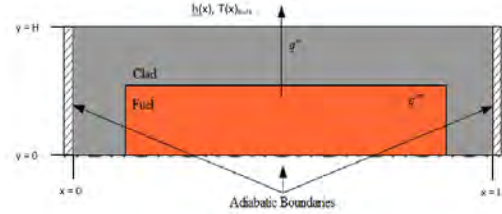


Figure 3. 2-D COMSOL Conduction Simulation Geometry

2.1 Simulation Physics

The governing equation for 2-D pure conduction with constant material properties and a distributed thermal source is Poisson's equation shown in Equation 1.

$$\frac{\partial^2 T(x, y)}{\partial y^2} = -\frac{q(x)'''}{k} \quad (1)$$

The details of the distributed power density in the fuel can be found in reference 3. The distribution data was entered into COMSOL and interpolated for use in the simulation. The boundary conditions specified in Figure 3 are formally written in Equation 2 and 3.

$$\frac{\partial T}{\partial x}\bigg|_{x=0} = \frac{\partial T}{\partial x}\bigg|_{x=L} = \frac{\partial T}{\partial y}\bigg|_{y=0} = 0 \quad (2)$$

$$\frac{\partial T}{\partial y}\bigg|_{y=H} = -\frac{h(x)}{k} [T(x, H) - T(x)_{bulk}] \quad (3)$$

Here the boundaries in Figure 3 corresponding to those in Equations 2 and 3 are labeled as follows:

1. $x = 0$, left most boundary
2. $x = L$, right most boundary
3. $y = 0$, bottom (symmetry) boundary

4. $y = H$, upper most boundary

The convection heat transfer coefficient data, $h(x)$, and the bulk temperature distribution data $T(x)_{bulk}$ were also entered into COMSOL and interpolated for use in the simulation. This data was imported from the SSHTC output file.

2.2 Simulation Results and Comparison

The COMSOL simulation results agree very well with those of the SSHTC. The clad surface heat flux results are shown in Figure 4 and the clad surface temperature results are shown in Figure 5. It is important to note that the clad surface temperatures are below the saturation point for the operational pressure mentioned in section 1.

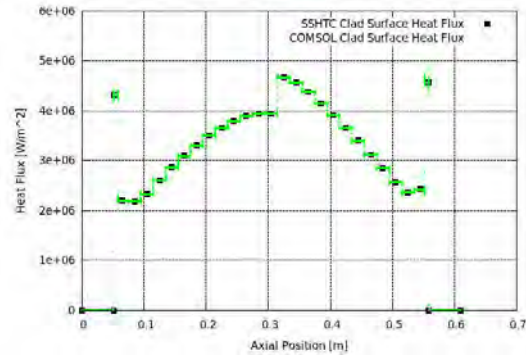


Figure 4. SSHTC- COMSOL Clad Surface Heat Flux Comparison.

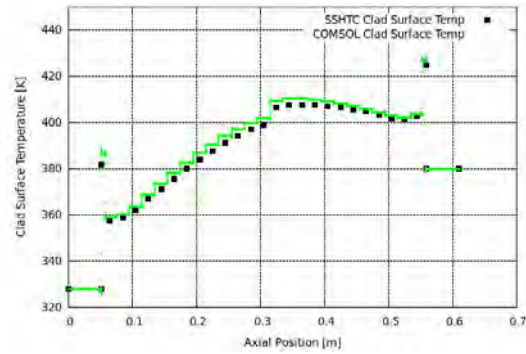


Figure 5. SSHTC-COMSOL Clad Surface Temperature Distribution.

3. Turbulent Conjugate Heat Transfer Simulation

Having shown that COMSOL can satisfactorily reproduce the SSHTC results, it was natural to investigate the thermal-hydraulic aspects of the system without the aforementioned simulation restrictions. This simulation couples the turbulent flow field with heat transfer in both the solid and fluid domains. By simulating the turbulent flow, the Nusselt number correlation was no longer needed to determine the quantity of thermal energy removed from the fuel plate. Instead the convection heat transfer is completely determined by the simulation physics, which provides a more physically accurate representation of the system. Also the thermal conductivity tensors in both the fuel and the clad were made isotropic to allow the diffusion of thermal energy in the axial direction of the CSG.

The CSG was modified to include a half coolant channel, i.e. 0.025 inches, fluid domain. The half coolant channel made use of the periodic boundary condition that naturally occurs in the center of the flow channel, which is also symmetric for the special case where the fuel is not contoured and the heat flux is equal on both sides of the fuel plate. The CSG for this simulation is shown in Figure 6.

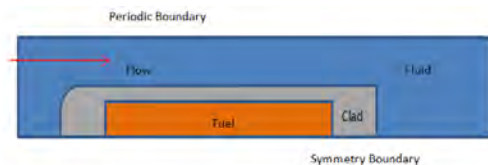


Figure 6. CSG for Turbulent Conjugate Heat Transfer Simulation. Note: Drawing not to scale.

The fluid domain has a 4.5 inch (0.1143 m) entrance length which was a necessary feature to accommodate the upstream adjustment of the flow field due to the flow obstruction presented by the fuel plate. The leading edge of the fuel plate was rounded off in accordance with the HFIR fuel plate geometry. Also, a 10 inch (0.254 m) downstream exit length was necessary to allow the fluid to completely expand downstream of the fuel plate. The exit length

was chosen to ensure that the exit pressure of the system was uniform.

Both the standard k- ϵ turbulence model and the low Reynolds number k- ϵ turbulence model (LRN) were coupled to the thermal energy diffusion equations for the fuel and the clad domains to simulate the fully turbulent convection heat transfer from the HFIR fuel plate. The standard k- ϵ model requires a wall offset, $\{y^+ | 30 \leq y^+ \leq 100\}$, in order to comply with experimental data. As a result of the wall offset, the momentum and thermal phenomena in the viscous sublayer of the turbulent boundary layer are not represented in the simulation. The LRN, on the other hand, does not require a wall offset, but instead, simulates flow conditions in the entire fluid domain including the viscous sublayer of the turbulent boundary layer [4].

At the inlet, the fluid has a uniform velocity and temperature distribution with magnitudes of 26.1 fps (7.94 m/s) and 128.9 °F (327 K), respectively. The fluid exit condition was set to a convective uniform pressure distribution with the pressure magnitude set to 0 Pa. The remaining exterior boundaries provide a symmetry condition, i.e. no thermal or momentum flux crosses the boundary. The interior boundaries of the system provide thermal continuity between the system constituents.

3.1 Simulation Results

The clad surface temperature profile for both the standard k- ϵ and the LRN are shown in Figure 7 compared with the temperature profile produced by the SSHTC. The turbulence models produced both lower clad surface temperatures and shallower axial clad surface temperature gradients than the SSHTC. The decrease in the temperature magnitude along the clad surface is an effect of the relatively large thermal gradients in the boundary layer of the fluid due to the turbulent characteristics of the flow. This has the effect of increasing the value of the convection heat transfer coefficient. The axial surface temperature gradient smoothing effect is a direct consequence of the 2D isotropic thermal conductivities in the solid domains. In other words, the diffusion of the thermal energy in the

axial direction reduces the thermal gradient in the axial direction.

The differences observed between the standard k-ε model and the LRN are due to the use of the wall offset in the former case. The most noticeable of these differences is the smaller clad surface temperature magnitudes. The wall offset takes the computational fluid domain away from the solid-fluid interface by a measure of y^+ , and projects a linear velocity profile through the viscous sublayer to the artificially displaced fluid domain. While this procedure does respect the no slip condition, the linear velocity profile has the potential to overestimate the fluid velocity resulting in artificially low surface temperatures as seen in Figure 7.

The LRN brings the flow domain into the viscous sublayer, thus providing a more accurate representation of the velocity profile in this region of the turbulent boundary layer. Since the potential to overestimate the velocity is diminished, the temperature distribution along the solid surface will be higher. Even though the LRN does predict higher temperatures than the standard k-ε model, the maximum temperature obtained in the LRN simulation is approximately 17 K lower than the temperature predicted by the SSHTC at that same location, i.e. 0.05 m in Figure 7.

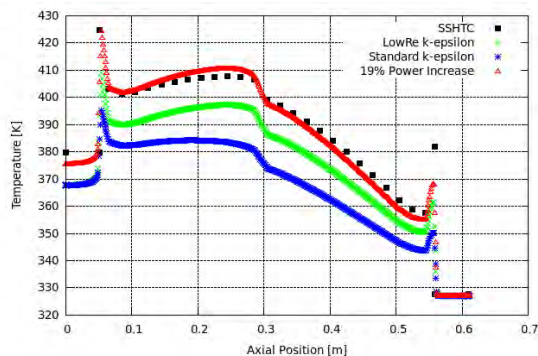


Figure 7. Clad Surface Temperature Comparison.

Confidence in the simulation results was increased by checking the global balances in mass and energy. The global mass balance was performed by calculating the relative error in the net integrated outflow of mass to that entering the system. This calculation yielded a value of 0% with 4 digit accuracy. The global balance of energy was performed by calculating the relative

error in the difference between the net integrated outflow of convected energy and the energy supplied to the flow from the fuel plate to the energy produced in the fuel meat. This calculation yielded a value of 1.748×10^{-2} %. Thus the simulation conserved these quantities very well.

Since the simulation temperature distribution was lower than that of the SSHTC, it was natural to inquire what increase in overall power density (PD) magnitude would bring the clad surface temperatures close to the SSHTC values. This value was approximated by comparing the difference in inlet temperatures to the outlet temperatures of both the SSHTC and the LRN simulation as shown in Equation 5.

$$PDP_{increase} \approx 1 - \frac{(T_{exit} - T_{inlet})_{LRN}}{(T_{exit} - T_{inlet})_{SSHTC}} \quad (5)$$

This calculation yielded a 19% increase. The comparison of the resultant temperature distribution with the SSHTC is shown to have good agreement in Figure 7.

4. Conclusions

The SSHTC uses the simulation restrictions described in section 1 to ensure that the HFIR core operates within the thermal limits of its material constituents. COMSOL was able to reproduce the thermal results of the SSHTC and thus proved its viability. Creating a more physically accurate simulation of the thermal-hydraulic phenomena encountered in the HFIR, using turbulent conjugate heat transfer model, demonstrated that the thermal margins have the potential to be reduced.

5. References

1. D.G. Morris and M. W. Wendel, "High Flux Isotope Reactor System RELAP5 Input Model", ORNL/TM-11647, Oak Ridge, TN (1993)
2. H.A. McLain, "HFIR Fuel Element Steady State Heat Transfer Analysis Revised Version", ORNL-TM-1904, Oak Ridge, TN (1967)

3. J.D. Freels, I.T. Bodey, R.V. Arimilli, K.T. Lowe, "Two-Dimensional Thermal Hydraulic Benchmark in Support of HFIR LEU Conversion using COMSOL", ORNL/TM-2010/018, Oak Ridge, TN (2010)

4. F.M. White, *Viscous Fluid Flow*. McGraw Hill, New York, NY (2006)

5. Ilas, G., Primm, R.T. "Fuel Grading Study on a Low-Enriched Uranium Fuel Design for the High Flux Isotope Reactor", ORNL/TM-2009/223/R1, Oak Ridge, TN (2009)

6. Acknowledgements

Research funded by the Department of Energy (DOE) Office of Science and the Global Threat Reduction Initiative (GTRI) of the National Nuclear Security Administration (NNSA) <http://nnsa.energy.gov/>

7. Appendix – LEU Geometry Creation

Any point on the base involute curve of the fuel plate can be found by specifying the subtended angle in the following equation, Equation A.1

$$\vec{r}_{inv} = |r| \{ i[\cos(\theta) + \theta \sin(\theta)] + j[\sin(\theta) - \theta \cos(\theta)] \} \quad (\text{A.1})$$

where $|r|$ is the radius of the involute generating circle and θ is the subtended angle. The terminal points of the linear sections of the LEU fuel contour, shown in Figure A.1, were determined by calculating their associated angular position along the base involute.

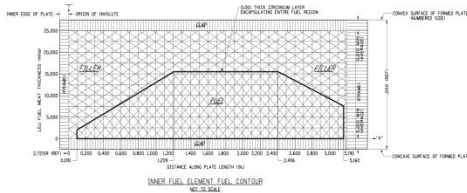


Figure A.1. Inner Fuel Element LEU Contour Relative to the Base Involute Curve.

Equation A.2 was used to determine this angular value.

$$\theta = \sqrt{\frac{2 \Delta s}{|r|}} \quad (\text{A.2})$$

Here Δs is the arc-length from the generating circle of the involute to the position of the terminal point for the LEU linear section. The arc-length, associated angle and height data are given in Table A.1. The arc-length and height data were harvested from reference 5.

Table A.1. LEU Fuel Contour Data

Arc-Length [in.]	Angle [rad]	Height [mils]
0.0909	0.25846	2.953
1.20945	0.942768	16.02
2.40551	1.32958	16.02
3.16024	1.52395	7.598

With these angular positions, one can form a piecewise continuous linear function for the heights of the LEU fuel contour above the base involute curve. The equation for the LEU contour section ranging from $0.25864 \leq \theta \leq 0.942773$ is

$$H_1(\theta) = \left(\frac{0.01602 - 0.002953}{0.942773 - 0.25864} \right) (\theta - 0.25864) + 0.002953 \quad (\text{A.3})$$

The equation for the LEU contour section ranging from $0.942773 \leq \theta \leq 1.32958$ is

$$H_2(\theta) = 0.01602 \quad (\text{A.4})$$

The equation for the LEU contour section ranging from $1.32958 \leq \theta \leq 1.52395$ is

$$H_3(\theta) = \left(\frac{0.007598 - 0.01602}{1.52395 - 1.32958} \right) (\theta - 1.32958) + 0.01602 \quad (\text{A.5})$$

With these equations one can modify the base involute equation, Equation 1, to place the LEU contour properly. This is done in the following manner: For an arbitrary section, the radial vector equation for the contour, \vec{r}_{con} , is

$$\vec{r}_{inv} = |r| \{ i[\cos(\theta) + (\theta + \alpha) \sin(\theta)] + j[\sin(\theta) - (\theta + \alpha) \cos(\theta)] \} \quad (\text{A.6})$$

where α is defined as

$$\alpha := \frac{H_n(\theta) + b}{|r|} \quad (\text{A.7})$$

Here the H_n represents the linear equations for the LEU fuel contour sections shown in Figure A.1 with $n = 1, 2,$ or 3 and explicitly given in Equations 3, 4, and 5. b is a parameter that allows the fuel meat contour to be placed anywhere normal to the base involute, e.g. 10 mils to allow for the clad in the HFIR fuel plate geometry. The LEU fuel meat contour place in the HFIR fuel plate involute geometry is shown in gray in Figure A.2.

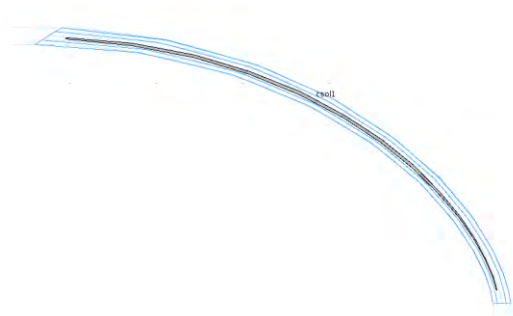


Figure A.2. Inner Fuel Plate with LEU Contour.